This value of valence bands offset matches with the published values for samples prepared in the in-situ conditions. The importance of the present method is that it is useful for samples prepared in ex-situ conditions with film thickness of the order of 100nm. This work was done in collaboration with a team from BARC.

(Contributed by: Shailendra Kumar, S.N. Jha, Jagannath, Tapas Ganguly, S.V.N. Bhaskara Rao, N.C. Das; shail@cat.ernet.in)

A.13 W/C X-ray multilayer mirror

X-ray multilayer devices consist of periodic arrangement of alternating layers of two different materials. The reflections of incident wave field from the successive interfaces in the multilayer add in phase at the Bragg condition and gives enhanced peak reflectivity. Smooth interfaces with chemical stability between the concerned materials are important prerequisites for making an ideal device. In x-ray mirrors, the interface roughness severely degrades the optics quality. Shape of the interfaces and their correlations and conformity with underneath layers are among the most important parameters. We have studied a W/C multilayer (C ~70Å/W ~40Å) by hard and soft x-ray reflectivity measurements. The hard x-ray reflectivity measurements are carried out using CuKα radiation (λ=1.54Å) and soft x-ray reflectivity measurement at λ=80Å using Indus-1 (fig. A.13.1 and fig. A.13.2). Detailed analysis of reflectivity data reveals that, in W/C multilayer, the roughness propagates across the successive layers from bottom to top layer. It is found that the roughness propagation factors for the two types of interfaces viz. W-on-C interface and C-on-W interface are different. In case of W-on-C interface the roughness propagation is slower in comparison to C-on-W interface. Amorphous carbon, which acts as a roughness suppresser, is responsible for asymmetric interface behavior. In fig.A.13.1 the best fit represented by continuous line is obtained by accumulated roughness model. The same model has been applied for the soft x-ray measurement and results are found in good agreement with hard x-ray data.

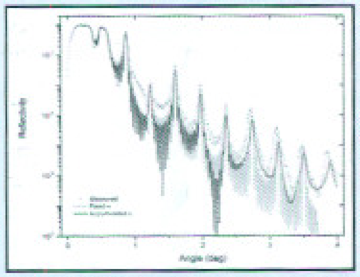

Fig. A.13.1 X-ray reflectivity spectra of W/C multilayer using λ=1.54Å wavelength is shown along with the fitted curve

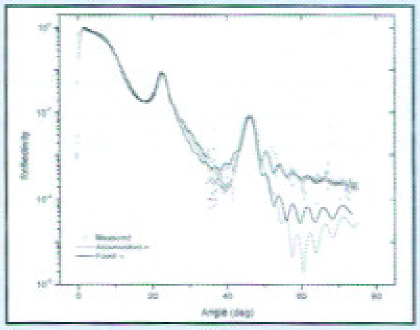

Fig A.13.2 X-ray reflectivity spectra of W/C multilayer at λ=80Å with the fitted curve.

(Contributed by: Dr. GS Lodha; lodha@cat.ernet.in))

A.14 Use of DC accelerator for radiation processing

A 750kV, 20kW DC electron accelerator designed and built at CAT, is currently being used to develop various processes relating to radiation processing of materials and food items. The beam from this electron accelerator provides an irradiation span 1.2 meters wide and (at 400keV) can penetrate 2mm deep in unit density material. The complete system is installed in a shielded area and is at present operating at 2.5kW power level, as permitted by the Atomic Energy Regulatory Board.

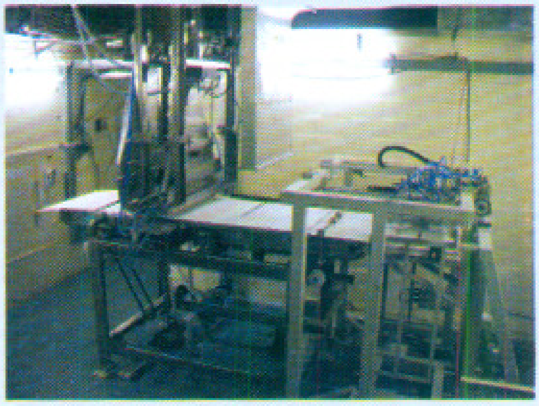

Fig.A.14.1 Irradiation of paper

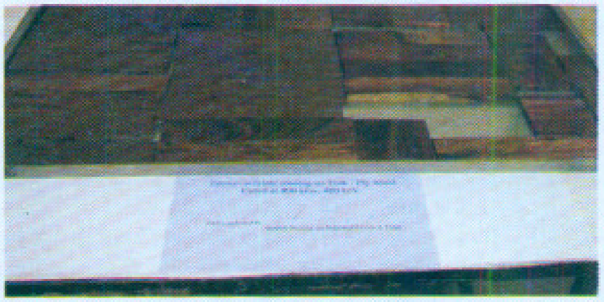

Fig. A.14.2 Irradiation of wood

The processes being developed and refined include surface irradiation of potatoes to prevent sprouting, disinfestations of seeds, de-polymerisation of paper pulp sheets, curing of coatings on wood and paints for value addition.

(Contributed by: SC Bapna; bapna@cat.ernet.in)

A.15 Injector control unit for 750kV DC Accelerator

The injector control unit for 750kV direct current accelerator consists of a filament power supply, which is floating at –750kV and a beam current stabilizing unit located at ground potential. The dc accelerator uses a directly heated diode gun as an electron emitter whose filament is a 0.3mm thick thoriated tungsten wire. A dc of 7 to 9A at about 2.5V suffices the filament for its complete range of emission. The accelerating voltage for 750kV dc accelerator is generated by a 15 stage voltage multiplier stack which is fed from a 22kV high frequency ac source The filament as well as emission current values are settable from the beam current stabilizing unit and the system operates either in constant filament-current mode or in constant emission mode depending on the signal, which overrides the other. The stimulus signal for controlling the ON/OFF periods of the power control-switch is transmitted to the filament power supply through an optical fiber link. The filament power supply generates a signal whose pulse-width is proportional to the filament current. This signal is then transmitted to the current stabilizing unit through another optical link where it is further processed to realize a feedback signal for the filament current. The return current of the high voltage generator gives the feedback signal for emission current.

The filament power supply is located inside the pressure vessel and it is floating at an extra high voltage of -750kV. Hence its reliability and MTBF requirements are extremely high because the failure of a single component inside the pressure vessel will cause a great loss of effort and time of the machine. Since the reliability of a system is adversely affected with the increase in component count, the main strategy in the design of this unit has been set to minimize the number of components floating at high potential and to protect them from high voltage transients in case of an arc. To meet the set objectives, the control electronics of the filament power supply is brought out of the pressure vessel by inserting a fiber optic link between the power supply and the beam current stabilizing unit. Only power components like rectifier diodes, switching MOSFET filter inductors and capacitors are kept floating at high potential. Input ac power to the filament supply is derived using a 1200: 1 step-down ferrite core transformer and a bulk converter scheme is employed to make the current controlled switched mode power supply for the filament.

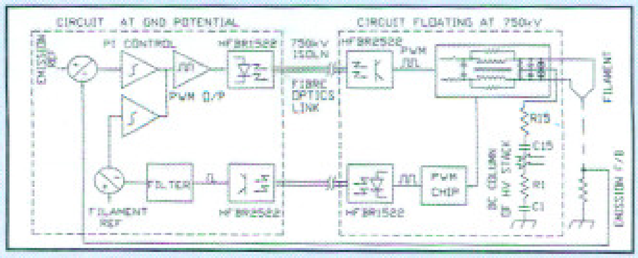

Fig. A.15.1 The schematic of the injector control unit

Fig. A.15.2 Filament power supply unit with high voltage dome removed

Fig.A.15.1 shows the complete schematic of the injector control unit. A high voltage dome fitted on the top of the stack provides an electrostatic shield to the filament supply unit as well as to the generator components. The output of the filament power supply is interfaced with the gun-filament through a high voltage common mode choke fitted with energy dissipating and surge arresting network consisting of glow discharge tubes and MOVs etc. The high voltage to the filament power supply is referred only at the gun end of this network with a solid copper strip of the shortest length. This helps in diverting the HV transients due to arcing in acceleration column directly to the DC column of the multiplier stack thus protecting the injector control unit. Fig.A.15.2 shows the filament power supply housing.

(Contributed by: R Banwari; rbn@cat.ernet.in)

A.16 Growth of CuO nanorods

Quasi one-dimensional nanostructures, such as nanowires and nanorods have attracted great attention during past few years due to their unique physical, chemical and electronic properties and for their potential applications in the field of nanodevices, field-emitters, and catalysts. We have carried out the synthesis of CuO nanorods by annealing a commercial grade Cu foil in oxygen atmosphere at high temperature. Our investigations reveal that the aspect ratio (the ratio of length to diameter of the nanorod) and density